Proceedings of IMECE2012
Proceedings of the ASME 2012 International Mechanical Engineering Congress & Exposition
November 9-15, 2012, Houston, Texas, USA

IMECE2012-86619

WAVE ENERGY EXTRACTION MAXIMIZATION USING DIRECT TRANSCRIPTION

James T. Allison, Allen Kaitharath, Daniel R. Herber
University of Illinois at Urbana-Champaign
Industrial and Enterprise Systems Engineering, Urbana, IL 61801
Email: {jtalliso,kaithar1,herber1}@illinois.edu

ABSTRACT

Wave energy converters (WECs) extract energy from the motion of ocean waves. A variety of different WEC devices have been studied over the past several decades, with emphasis on cost-effective energy extraction. Active control has been shown to improve energy production significantly. Here we investigate energy extraction potential of a tethered heaving cylinder WEC using direct transcription (DT), an open-loop optimal control strategy. This enables direct inclusion of asymmetric constraints on power and tether force, practical considerations not considered in previous studies, and opens the door to WEC optimal control problems with more realistic nonlinear models and integration of control design with physical system design.

1 Introduction

Energy extraction from ocean waves and conversion to electrical energy is a promising form of renewable energy, yet achieving economic viability of wave energy converters (WECs) has proven challenging. Numerous WEC designs have been investigated, particularly over the course of the last four decades (see [1] for early work). Reviews of available WEC technologies are available in [2–5]. In this article we focus on heaving cylinders tethered to a power take-off (PTO) moored to the ocean floor (Fig. 1), similar to the systems described in [6] and [7]. The vertical position of the mass center z is measured from the equilibrium position of the mass center in still water (z_{me}). The cylinder radius is r, and the wave elevation z_0 is measured from the still water level (SWL).

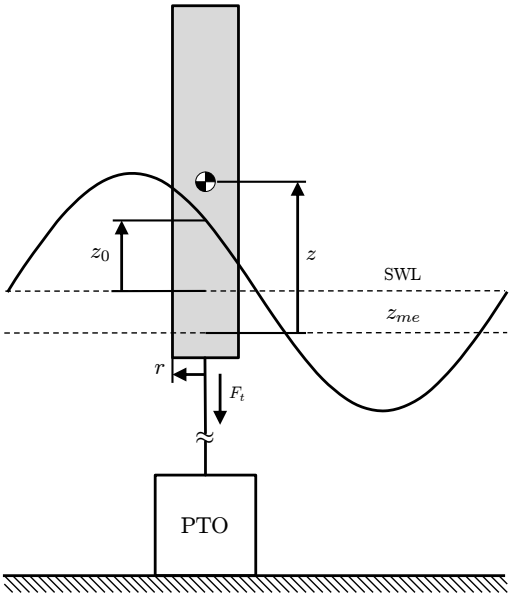

Figure 1: Tethered heaving cylinder wave energy converter.

As buoyancy forces the heaving cylinder upward, motion is resisted by the PTO via the mooring cable. Work is done on the PTO at the rate $P = F_t\dot{z}$, where F_t is the tether force and $\dot{z}$ is the vertical velocity of the heaving cylinder. Here we assume the body is constrained to vertical motion. In systems that use a cable tether, F_t must remain non-negative; this requirement can be maintained either through tether pretension or active control. We will

also explore the case where a rigid tether allows compression ($F_t < 0$), although buckling limits this type of system to shallow water installations.

While passive WECs can produce energy, incorporating active control increases significantly energy production capability [8, 9], increasing economic competitiveness. Falnes and Budal used frequency domain analysis to derive optimality conditions for point absorbers (heaving body WECs that are much smaller than ocean wavelength λ and have only one mode of oscillation) based on several simplifying assumptions, including linearity and regular monochromatic ocean waves [10, 11]. Falnes and Budal treated velocity $\dot{z}$ as an independent control input; while velocity is an impractical control signal, it simplifies solution of optimal control problems. Falnes reasoned that given an optimal velocity trajectory, the corresponding control force (F_t) could be derived. The optimality velocity trajectory is given by:

$$\hat{\dot{z}}_* = \frac{\hat{F}_e}{2R} \tag{1}$$

where $\hat{\dot{z}}_*$ is the complex amplitude of the velocity trajectory, $\hat{F}_e$ is the excitation force, and R is the radiation resistance (the real part of the WEC radiation impedance, which depends on WEC geometry [11]). This indicates that, under the above assumptions, velocity must be in-phase with excitation force for maximum power production. For point absorbers, excitation velocity is approximately in phase with wave elevation $z_0(t)$. If these optimality conditions are met, the maximum power production is:

$$P_{\max} = \frac{|\hat{F}_e|^2}{8R} = \frac{1}{2}P_{e*}, \tag{2}$$

indicating that at most a point absorber with a single oscillation mode can absorb one-half of the available wave power: $\frac{1}{2}P_{e*}$. One implication of Eqn. (1) is that maximal power production requires a reactive control system, i.e., optimal energy extraction requires a PTO capable of injecting power into the system, rather than just extracting it. Bi-directional power flow helps exploit natural WEC dynamics [12–14] to maximize power production. Unfortunately PTOs capable of bi-directional power flow are difficult to implement in practice, but without reactive control WEC energy extraction is suboptimal.

Wave energy extraction can be increased further by designing a WEC such that it resonates with incoming waves, similar to the behavior of electromagnetic antennae or acoustic microphones [11]. The natural frequency of a heaving point oscillator is given by:

$$\omega_0 = \sqrt{\frac{k_b}{m + m_a}} \tag{3}$$

where k_b is the hydrostatic stiffness, m is the heaving body mass, and m_a is the added mass that arises from the motion of radiated waves. Hydrostatic stiffness is a useful model for buoyancy that is analogous to mechanical mass-spring systems. For heaving bodies with a constant cross-section, the upward buoyancy force is proportional to submersion depth. If z in Fig. 1 is measured from the equilibrium position of the mass center position in still water, gravitational force drops out from net force calculations, and the buoyancy force can be written:

$$F_b = \pi\rho r^2(z - z_0) = k_b(z - z_0) \tag{4}$$

where $\rho = 1{,}020$ kg/m^3 is the sea water density and $k_b = \pi\rho r^2$ is the hydrostatic stiffness. The added mass is $m_a = \frac{4}{3}\rho r^3$ [15], which can be neglected if the draught (i.e, the submerged length: $\ell = m/\rho\pi r^2$) is much larger than the heaving cylinder's radius [11]. In this case the natural frequency can be simplified to:

$$\omega_0 \approx \sqrt{\frac{k_b}{m}} = \sqrt{\frac{g}{\ell}} = r\sqrt{\frac{g\rho\pi}{m}},$$

and we can see that natural frequency increases with radius r and decreases with m.

If WEC natural frequency matches the incoming wave frequency, i.e., $\omega_0 = \omega_w$, a resonant condition results that amplifies WEC response and power production. Often in WEC development the physical design and control design are addressed together (at least informally) to produce a WEC system with appropriate dynamic stiffness and robust energy production performance. This design approach is an ad hoc form of co-design, a class of design methods for integrated physical and control system design that often leads to significant performance improvements [14, 16–18].

If real ocean waves were monochromatic (constant ω_w), WEC design would be straightforward; WECs could be developed to resonate at the unchanging incoming wave frequency. Unfortunately real ocean waves are polychromatic, and WEC resonant response typically is much more narrow than ocean wave spectra [9, 19]. Power production may be improved by either enhancing performance under off-resonance conditions, or providing the means to change dynamically WEC resonance properties to match dominant wave conditions [20]. Both approaches are significant challenges in WEC design.

1.1 Wave Energy Converter Control

WEC dynamic response and energy production performance can be controlled via the tether force connecting the heaving cylinder to the PTO. The PTO converts reciprocating linear motion to electrical energy using one of several mechanisms. Ivanova et al. investigated the effectiveness of a linear electric generator [21], while a more common approach is to use the tether to drive a hydraulic system that powers a hydraulic motor connected to a rotational genera-

tor [22–26]. The hydraulic system can provide a more even rotational velocity to the generator, and provides superior flexibility in control force possibilities, but suffers from low transmission efficiency.

An effective WEC control system boosts power production in off-resonance conditions. One intuitive approach proposed by Budal and Falnes [10] involves 'latching' the system in place when $\dot{z} = 0$ for a short period. This allows the motion of the waves to 'catch up' to the motion of the heaving cylinder before releasing again (if $\omega_0 > \omega_w$). The objective of latching control, sometimes referred to as phase control [11, 22, 24, 26], is to keep $\dot{z}$ and F_e in phase (or at least to align the extrema of these trajectories with respect to time). This strategy is based on the phase requirement for reactive control presented in Eqn. (1).

Latching can be implemented using hydraulic valves or mechanical brakes [26,27]. The dwell time between latching and release is a critical control design decision. Clement and Babarit confirmed the optimality of Falnes' original latching control strategy, with respect to a set of assumptions, by applying Pontryagin's Maximum Principle [9, 28]. Clement further showed that a hybrid latching and declutching (freewheeling) control strategy amplified power production substantially, increasing it beyond the sum of the two strategies individually.

In addition to reactive, latching, and declutching control, a variety of other control strategies have been explored, including model predictive control (MPC) [29], multiple power-point tracking (a strategy often used in solar energy systems) [30], PID [31], and feedback linearization [31].

1.2 Optimal Power Production

Under narrow assumptions, conditions for maximal power production can be derived analytically. According to Eqn. (1), $\dot{z}$ and F_e must be in phase. While the F_t trajectory required to produce $\dot{z}_*$ can be calculated, it may not always be practical to implement. If we assume a simple impedance model for the PTO:

$$\hat{F}_t = -Z_t \hat{\dot{z}} = -(R_t + X_t)\hat{\dot{z}} \tag{5}$$

where R_t is the real part (resistance) and X_t is the imaginary part (reactance) of the PTO impedance Z_t, we can define an optimal control strategy that maximizes energy extraction. If $Z_i = R_i + X_i$ is an impedance model for the heaving cylinder, the optimal control is given by $Z_{t*} = Z_i^*$, where Z_i^* is the complex conjugate of Z_i. Here X_t is non-zero so that it can cancel out X_i, meeting the phase conditions defined in Eqn. (1). This strategy is known as reactive control, since the control reactance X_t is non-zero [26]. This implies that F_t is harmonic, and when compared against the $\dot{z}$ trajectory it is clear that power $P = F_t \dot{z}$ will not have a restricted sign, meaning power must flow both directions. Constructing a PTO capable of reactive power flow is one of several significant impediments to achieving exact optimal reactive control [9].

Latching control was introduced to help satisfy the phase condition even in the presence of variable wave frequency. While this has proven to be an implementable technique, it is a suboptimal control strategy [9, 24]. If we impose latching control, we can still calculate the best possible release time [9,32], but the results are limited by this control structure and will not perform as well as reactive control.

Both standard reactive control and latching control are non-causal, preventing exact real-time implementation without accurate incoming wave prediction. For latching control, if the wave elevation is uncertain (i.e., irregular waves with imperfect prediction), then the latching release time will be suboptimal. Demonstration of accurate wave prediction is an important recent advancement [26]. In addition, suboptimal methods for causal reactive control have been developed that approximate optimal results [33].

In most previous derivations of optimal WEC control, velocity has been treated as an independent control input (e.g., [11, 26, 29]). While this may not make physical sense (it is a state!), this approach can be useful. If we seek to maximize energy production, it is possible to formulate the optimal control problem such that the control input (velocity) appears quadratically in the Hamiltonian, meaning that the resulting optimal control problem is not singular. This aids solution, but velocity is not a realistic independent control variable.

In an actual WEC system a voltage signal to the PTO generator or a hydraulic control valve influences the actuation force on the buoy, which in turn influences the velocity. While we can backsolve for the required force required to produce the 'optimal' velocity trajectory, the PTO may not be capable of providing this force. A more realistic approach would include a dynamic PTO model and use the voltage input as the control input. Here we propose an intermediate approach where we neglect PTO dynamics and treat the tether force as the independent control variable. While this is a significant approximation, tether force is qualitatively more appropriate to use as a control input. In addition, we can now place constraints directly on F_t reflective of realistic PTO devices. Unfortunately, with this problem formulation, F_t appears linearly in the Hamiltonian:

$$H(\boldsymbol{\xi}, \boldsymbol{\lambda}, u, t) = \boldsymbol{\lambda}^{\mathrm{T}}(t)\left(\mathbf{A}\boldsymbol{\xi}(t) + \mathbf{B}u(t)\right) + u\xi_2(t) \tag{6}$$

where $\boldsymbol{\xi} = [z, \dot{z}]^{\mathrm{T}}$ is the state vector, $u = F_t$ is the control input, $\boldsymbol{\lambda}$ is the costate vector, and $\mathbf{A}$ and $\mathbf{B}$ define the linear time-invariant model of the heaving cylinder. Consequently, maximizing energy production with respect to $F_t(t)$ is a singular optimal control problem (which is difficult, but possi-

ble to solve).

Clement and Babarit formulated WEC control as a singular optimal control problem and solved it using Pontryagin's Maximum Principle [9]. Rather than treating F_t as the control input, they modeled the PTO generator as a simple linear damper with rate b_1. Latching capability was provided by connecting in parallel with the first damper an extremely stiff damper with rate $b_2 \gg b_1$. The total damping rate was a linear combination of these two rates $(b_1 + ub_2)$, where $u \in [0,1]$ allowed control over damping rate. The WEC is fully latched when $u = 1$. Clement and Babarit derived an analytical solution to this optimal control problem, which resulted in simple latching rules and bang-bang control behavior (u switches between 0 and 1), which is expected because the problem was singular. In the following sections we will present an alternative singular problem formulation that places no restrictions on PTO structure and allows for solutions with singular arcs (i.e., not bang-bang control).

Energy production is not the only possible objective function for WEC design. Falnes proposed using the power-to-volume ratio as an alternative objective function, reasoning that the swept volume of a heaving body is proportional to cost, and the primary goal is designing WECs that reduce cost per unit of energy produced [11]. While the accuracy of volume as a cost proxy may be debated, an interesting result of this analysis is the recommendation that large arrays of small WECs are more cost effective than small arrays of large WECs [26, 34]. The maximum recommended WEC size depends on sea state data for a particular location [26]. If WEC arrays are spaced closely, inter-WEC interaction should be included in analysis. Also, the phase requirement described above is not valid for closely-spaced WEC arrays [35]. De Backer et al. argue that computational fluid dynamics is required to properly predict the performance of closely-spaced arrays [36]. These results point to the need for system-level design for wave energy conversion. In addition to developing well-designed individual WECs, these designs should be congruent with the needs for the overall system when arrays are used.

1.2.1 PTO Models Based on the optimal reactive control described above, maximal energy extraction is achievable if a PTO has dynamic behavior described by Eqn. (5) with appropriately tuned parameters. Such a PTO has a dissipative term (R_t) and a capacitive term (X_t). This motivates modeling a PTO as a linear spring-damper system:

$$F_t = zk_p + \dot{z}b_p \tag{7}$$

where the PTO stiffness k_p corresponds to the capacitive term and the PTO damping b_p corresponds to the dissipative term. Assuming monochromatic wave input, and that k_p and b_p can be tuned, a PTO design of this form can be identified that maximizes energy extraction [9].

While the model in Eqn. (7) is widely used [9,24,25,27], the PTO is limited to a harmonic force trajectories, and these dynamics are not reflective of realistic PTO generators. Realistic PTOs are highly nonlinear, invalidating frequency domain analysis (e.g., [10, 11]); linear spring-damper models are significant idealizations [24]. Clement and Babarit did introduce a model that accounted for dynamic response in b_p adjustment, but no previous WEC optimal control studies have included a realistic dynamic PTO model. The typical linear PTO model oversimplifies practical challenges, such as power flow or force constraints. In this article we propose an open-loop optimal control technique that treats F_t as an independent control input and does not constrain it to harmonic trajectories, eliminating the need to assume a PTO design architecture while enabling non-harmonic/nonlinear solutions and the inclusion of constraints directly on F_t.

1.2.2 Power and Force Constraints Practical constraints on power flow and tether force have been addressed rarely in the literature. Halls and Falnes imposed symmetric tether force constraints [29], but in practice asymmetric constraints (e.g., $0 \leq F_t \leq F_{\max}$) are more appropriate. Often no explicit F_t constraints are imposed.

Practical PTOs (at least so far) cannot provide bi-directional power flow [11]. Studies that use the linear spring-damper PTO model described above often impose this power constraint by eliminating the reactive term (i.e., $k_p = 0$). Energy extraction in this case is assumed to behave exactly as a linear damper, which is convenient for modeling, but does not reflect accurately the behavior of a real PTO. Another more practical approach to impose the power flow constraint is latching control; locking the PTO over specific periods can maintain unidirectional power flow without unrealistic assumptions of PTO characteristics. Declutching (disconnecting the PTO temporarily) can also help satisfy the power constraint.

Whether using a damping model or implementing latching control, each case makes significant assumptions about the nature of the WEC system, resulting in a suboptimal solution. We need an approach that allows us to solve for optimality without unnecessary design limitations imposed by assumptions to simplify analysis. In this article we propose an alternative WEC analysis and design approach that makes no assumptions regarding PTO structure, allows for nonlinear models, and enables direct constraints on force,

power, and other quantities. In other words, it enables us to solve the problem that we want to solve directly.

1.3 Direct Transcription

Several distinct approaches have been applied to solving the optimal control problem for WEC energy maximization. Early work focused on frequency domain techniques that allowed analytical solutions, but these were based on significant simplifying assumptions regarding the WEC system and the sea state. Heuristics, such as latching or declutching control, help solve several practical WEC system design issues, but produce suboptimal results. A handful of studies employed an 'optimize then discretize' (O→D) approach, where Pontryagin's Maximum Principle is applied to derive a boundary value problem (BVP) based on a time-domain representation of the system. If the BVP cannot be solved analytically it can then be discretized and solved numerically (hence O→D).

Another class of methods is known as 'discretize then optimize' (D→O). Here the time domain representation of the system is discretized first using a collocation method. The system can then be optimized in one of two ways. The first, known as single-shooting [37] or multidisciplinary feasible (MDF) [18, 38], uses a nested process where an outer loop nonlinear programming algorithm solves the optimization problem with respect to discretized control inputs, and for every function call made by the optimization algorithm the inner loop simulates the discretized system equations using a forward simulation algorithm (e.g., a Runge Kutta algorithm).

Consider the following general optimal control problem:

$$\begin{aligned} \min_{\boldsymbol{\xi}(t),\mathbf{u}(t),t_F} \quad & \int_0^{t_F} L(\boldsymbol{\xi}(t),\mathbf{u}(t),t_F)dt \\ \text{subject to:} \quad & \dot{\boldsymbol{\xi}} = \mathbf{f_d}(\boldsymbol{\xi}(t),\mathbf{u}(t),t) \end{aligned} \tag{8}$$

where $\boldsymbol{\xi}$ is the state vector, $\mathbf{u}$ is the control vector, t_F is the potentially variable end time, and $\mathbf{f_d}(\cdot)$ is the derivative function. Initial state conditions $\boldsymbol{\xi}(0) = \boldsymbol{\xi}_0$ are imposed, and algebraic equality or inequality constraints may be included. In an MDF formulation we discretize the differential equations (differential algebraic if applicable) using a collocation method and solve these equations using forward simulation for each optimization algorithm function call. For example, if we hold t_F constant, the MDF formulation of Prob. (8) is:

$$\min_{\mathbf{U}} \quad \sum_{i=1}^{n_t-1} L(\boldsymbol{\xi}_i,\mathbf{u}_i)h_i \tag{9}$$

where $\mathbf{U}$ is a discretized matrix representation of the control trajectories $\mathbf{u}(t)$ (the ith row of $\mathbf{U}$ is $\mathbf{u}_i = \mathbf{u}(t_i)$, $i = 1,2,\ldots,n_t$), h_i is the ith time step ($h_i = t_{i+1} - t_i$), n_t is the number of time steps (including both end points), and $\boldsymbol{\xi}_i = \boldsymbol{\xi}(t_i)$, $i = 1,2,\ldots,n_t$. Each $\boldsymbol{\xi}_i$ must satisfy the state equations discretized using collocation. For example, if the trapezoidal collocation method is used in solving Prob. (9), the following system of equations is solved for $\boldsymbol{\Xi}$ (the matrix whose rows are $\boldsymbol{\xi}_i$) using forward simulation for each given value of $\mathbf{U}$ provided by the optimization algorithm:

$$\begin{aligned} \boldsymbol{\xi}_{i+1} = \boldsymbol{\xi}_i + \frac{h_i}{2}\left(\mathbf{f_d}(\boldsymbol{\xi}_i,\mathbf{u}_i,t_i) + \mathbf{f_d}(\boldsymbol{\xi}_{i+1},\mathbf{u}_{i+1},t_{i+1})\right), \\ i = 1,2,\ldots,n_t-1 \end{aligned} \tag{10}$$

MDF has fewer limitations than the O→D approaches. The system model can be nonlinear, and inequality path constraints may be imposed directly on states, control inputs, or functions of these quantities. In O→D approaches analytical derivatives of the Hamiltonian are required (limiting the type of problems that can be solved), but these are not needed in MDF. With D→O approaches we convert the infinite dimensional optimization problem to a finite dimensional nonlinear program (NLP).

The second D→O approach, known as Direct Transcription (DT) [37,39] or All-at-Once (AAO) [18,38], avoids nested simulation by including the collocation equations directly as optimization constraints, eliminating the need for nested simulation:

$$\begin{aligned} \min_{\mathbf{U},\boldsymbol{\Xi}} \quad & \sum_{i=1}^{n_t-1} L(\boldsymbol{\xi}_i,\mathbf{u}_i)h_i \\ \text{subject to:} \quad & \boldsymbol{\zeta}(\mathbf{U},\boldsymbol{\Xi}) = -\frac{h_i}{2}\left(\mathbf{f_d}_i + \mathbf{f_d}_{i+1}\right) \\ & \qquad + \boldsymbol{\xi}_{i+1} - \boldsymbol{\xi}_i = \mathbf{0} \\ & i = 1,2,\ldots,n_t-1 \end{aligned} \tag{11}$$

where the collocation equations rearranged into null form are termed defect constraints: $\boldsymbol{\zeta}(\mathbf{U},\boldsymbol{\Xi}) = \mathbf{0}$. While DT results in a large dimension optimization problem, its structure can be exploited for efficient solution. Additionally, DT is capable of solving difficult singular optimal control problems, unstable control problems, and problems with inequality path constraints. It places no unnecessary constraints on solution trajectories, and is applicable to challenging nonlinear problems, including WEC control problems with tether force and power constraints. DT also can solve for time-independent parameters, enabling efficient solution of combined optimal control and physical design problems [18].

In cases where the objective function integrand $L(\cdot)$ is quadratic and the dynamic system model is linear, the DT problem can be formulated as a quadratic program (QP), leading to especially efficient solution. At times a nested solution approach (MDF) leads to pathologically difficult optimization problems (multi-model, non-convex), while a well-crafted DT formulation of the same problem has a high

dimension but is very easily solved (convex, or at least well-behaved). Hals and Falnes implemented a DT-like solution to WEC optimal control (including a QP formulation), although velocity was treated as the independent control input, so the resulting optimal control problem was not singular [29].

2 Point Absorber Design

Here we explore the design of a heaving cylinder WEC (Fig. 1), both from a control and a physical design perspective, using DT. Power and asymmetric tether force constraints are considered explicitly; four distinct cases are studied:

Case 1) No constraints on tether force ($F_t \in \mathbb{R}$) or power ($P \in \mathbb{R}$)
Case 2) Non-negative tether force ($F_t \in \mathbb{R}_{\geq 0}$), no power constraint ($P \in \mathbb{R}$)
Case 3) No constraints on tether force ($F_t \in \mathbb{R}$), non-negative power ($P \in \mathbb{R}_{\geq 0}$)
Case 4) Non-negative tether force ($F_t \in \mathbb{R}_{\geq 0}$), non-negative power ($P \in \mathbb{R}_{\geq 0}$)

In this section the system model is described in more detail, the DT implementations for all four cases are presented, and numerical results and design implications are discussed.

2.1 System Model

Here the heaving cylinder WEC is modeled as a point mass subject to three forces: buoyancy (Eqn. (4)), tether force (control input), and a linear damping force ($F_d = b(\dot{z} - \dot{z}_0)$) that was included to account for viscous losses from the WEC oscillating in seawater. The damping coefficient b was calculating by linearizing a quadratic viscous drag model for a blunt nose cylinder with a large aspect ratio, i.e., $\ell/2r \gg 2$, implying that the drag coefficient is approximately 0.81 [40]. Assuming the upper limit for velocity is $\dot{z}_{\max} = 15$ m/s, the linearized damping force can be written as:

$$F_d = \frac{C_D \rho \pi r^2}{2\dot{z}_{\max}} (\dot{z} - \dot{z}_0) = b(\dot{z} - \dot{z}_0) \tag{12}$$

and the equation of motion for the heaving cylinder is:

$$m\ddot{z} + k_b(z - z_0) + b(\dot{z} - \dot{z}_0) - F_t = 0. \tag{13}$$

Here we assume the wave trajectory exciting the WEC is monochromatic under deep sea wave conditions with amplitude $a = 2$ m and frequency $f = 1/8$ Hz: $z_0 = a\sin(2\pi f t)$. The wavelength can be computed to be $\lambda = 100$ m. Added mass is neglected since $\lambda \gg r$ [11]. A state space representation of this system is:

$$\dot{\boldsymbol{\xi}} = \mathbf{A}\boldsymbol{\xi} + \mathbf{B}\mathbf{u} \tag{14}$$

where:

$$\mathbf{A} = \begin{bmatrix} 0 & 1 \\ -k_b/m & -b/m \end{bmatrix} \quad \mathbf{B} = \begin{bmatrix} 0 & 0 & 0 \\ -k_b/m & -b/m & -1/m \end{bmatrix}$$

$$\boldsymbol{\xi} = \begin{bmatrix} z \\ \dot{z} \end{bmatrix} \qquad \mathbf{u} = \begin{bmatrix} z_0 \\ \dot{z}_0 \\ F_t \end{bmatrix}$$

In this study we seek to identify the control force trajectory $F_t(t)$ that maximizes energy production for this WEC. Referring to Eqn. (8), the objective function is:

$$\int_0^{t_F} \dot{z}(t) F_t(t) dt$$

and the state space constraint is given by Eqn. (14). Observe that the control input $u(t) = F_t(t)$ appears only linearly in both the objective and constraint, and hence also in the Hamiltonian. Therefore, this is a singular optimal control problem. Fortunately, DT is an effective methodology for solving singular optimal control problems, even in the presence of singular arcs (i.e., beyond bang-bang control) [39]. Additionally, DT allows for the inclusion of inequality path constraints. In Case 4 described above, both power and tether force constraints are added to the optimization problem:

$$F_t(t) \geq 0 \tag{15}$$

$$\dot{z}(t) F_t(t) \geq 0 \tag{16}$$

These constraints may change activity between $t = 0$ and $t = t_F$ ($= 48$ seconds here). When active, an algebraic constraint is effectively added to the system equations, converting them from ordinary differential equations to a system of differential algebraic equations (DAEs) [41]. With conventional optimization approaches, determining when inequality path constraints come in and out of inequality is difficult, whereas DT handles path constraints naturally.

The first step in applying DT is to discretize the problem. Here we use a fixed step size: $h = t_F/(n_t - 1)$ ($t_1 = 0$ s, and $t_{i+1} = t_i + h$), and apply the trapezoidal collocation method presented in Eqn. (10). If $n_s = 2$ is the number of state variables, this results in $n_s \times n_t$ defect constraints. If $n_c = 1$ is the number of control inputs, the dimension of the optimization variables for Eqn. (11) (i.e., $\mathbf{U}$ and $\boldsymbol{\Xi}$) is $n_c \times (n_t - 1) + n_s \times (n_t - 1)$.

While often DT solves singular control problems effectively without deviation from standard implementations, the WEC problem required a few modifications. Cases 3 and 4 with the nonlinear power constraints proved to be more challenging to solve than the first two cases. One change that improves DT efficacy for singular optimal con-

trol problems is to increase the time step size for control inputs [37]. This allows for the control input to adapt after the states have a short period of time to evolve. Here we define the control step size as $h_c = \kappa h$, where κ is a positive integer. Observe that when $\kappa > 1$, this modification reduces the dimension of $\mathbf{U}$; the number of control time steps is $n_u = \frac{n_t - 1}{\kappa} + 1$.

A second modification required for Cases 3 and 4 was to add a small quadratic control effort term to the objective function: $RF_t(t)^2$, where R is a small scalar [37]. While a large value of R increases distance from singularity, it changes the optimization problem, so the smallest value of R that results in successful problem solution is desirable.

After discretization and application of the above two modifications, the DT problem implementation for Case 4 is:

$$\begin{aligned} \min_{\mathbf{U},\boldsymbol{\Xi}} \quad & -h \sum_{i=1}^{n_t-1} \left(\dot{z}_i F_{t,j} - R F_{t,j}^2 \right) \\ \text{subject to:} \quad & \boldsymbol{\zeta}(\mathbf{U},\boldsymbol{\Xi}) = -\frac{h_i}{2}\left(\mathbf{f}_{\mathbf{d}\,i} + \mathbf{f}_{\mathbf{d}\,i+1}\right) \\ & \qquad + \boldsymbol{\xi}_{i+1} - \boldsymbol{\xi}_i = \mathbf{0} \\ & -F_{t,j} \le 0 \\ & -\dot{z}_i F_{t,j} \le 0 \\ \text{where} \quad & i = 1, 2, \ldots, n_t, \quad j = \left\lfloor \frac{i - 1 + \kappa}{\kappa} \right\rfloor, \end{aligned} \tag{17}$$

and $\mathbf{f}_{\mathbf{d}\,i} = \mathbf{f}_{\mathbf{d}}(\boldsymbol{\xi}_i, t_i) = \mathbf{A}\boldsymbol{\xi}_i + \mathbf{B}\mathbf{u}_i$. Observe that the objective function is a quadratic function of optimization variables, and for Cases 1 and 2, all constraints are linear. Consequently, for these two cases, Prob. (17) can be solved using efficient quadratic programming (QP) algorithms [42]. In Cases 3 and 4, a large number of quadratic constraints are included (a power constraint at each time step) making the problem a quadratically-constrained quadratic program (QCQP). If a general nonlinear programming (NLP) algorithm applied, the solution may still be obtained efficiently since analytical derivatives are obtained easily and the sparse problem structure may be exploited in matrix calculations. In more general cases where analytical derivatives are unavailable, DT implementations can still be solved efficiently by exploiting the sparse constraint Jacobian structure and using sparse finite difference derivative approximations [39].

2.2 Numerical Results

The direct transcription problems for all four cases were solved using the parameter values listed in Table 1. Parametric studies were also performed on discretization resolution and WEC mass.

2.2.1 Direct Transcription Results

DT results are summarized in Fig. 2. The initial state used was $\boldsymbol{\xi}_0 = [0, 0]^{\mathrm{T}}$, and in each case a steady-state oscillatory trajectory was achieved after about one period of the wave. The top row of Fig. 2 illustrates the position (solid line), velocity (dashed line), and tether force (dot-dash line) for each of the four cases, and the bottom row of the figure shows the instantaneous power trajectories (i.e., $P = \dot{z}F_t$) for each case. A single eight second period, between 24 and 32 seconds, is shown instead of the full simulation for better visualization.

In all four cases power at 26 and 30 seconds is zero; note that at these two time instants the tether force is zero. Power below the zero line in these plots is reactive power, i.e., power must flow from the PTO to the heaving cylinder. The maximum power peak for Cases 2-4 is approximately the same (525 W), while the wider peaks from Case 1 lead to greater overall energy production. Total energy extraction for each of the four cases is:

Case 1	Case 2	Case 3	Case 4
1470 J	724 J	1400 J	703 J

The unconstrained case, as expected, produced the most energy. Removing the tether force constraint clearly has a larger impact on energy production than removing the power constraint. In Cases 2 and 4 we observe regions where the tether force is flat at zero. This is analogous to the declutching behavior described previously in other WEC systems. During these periods the heaving cylinder 'rides' the wave down passively until positive force is capable of resisting cylinder motion and producing power. These flat regions are necessary in these two cases to satisfy the tether force constraint (i.e., the PTO cannot push on the cylinder).

In Case 3 the tether force has no flat spots, indicating that declutching is not desirable when not required by tether force constraints. The velocity, however, does have flat spots; this is analogous to latching control. Just the right amount of force is provided to produce zero velocity in two regions. Observe the symmetry of the two latching regions; the first occurs while the buoy is at its maximum position, just before it descends to it's lowest position where it is latched again. During this descent the cylinder achieves its maximum negative velocity, and passes through its point of maximum power output.

Table 1: WEC and Direct Transcription Parameters.

m	20 kg	n_t	1393
r	0.2 m	R	0.004
ρ	1020 kg/m^3	κ	2

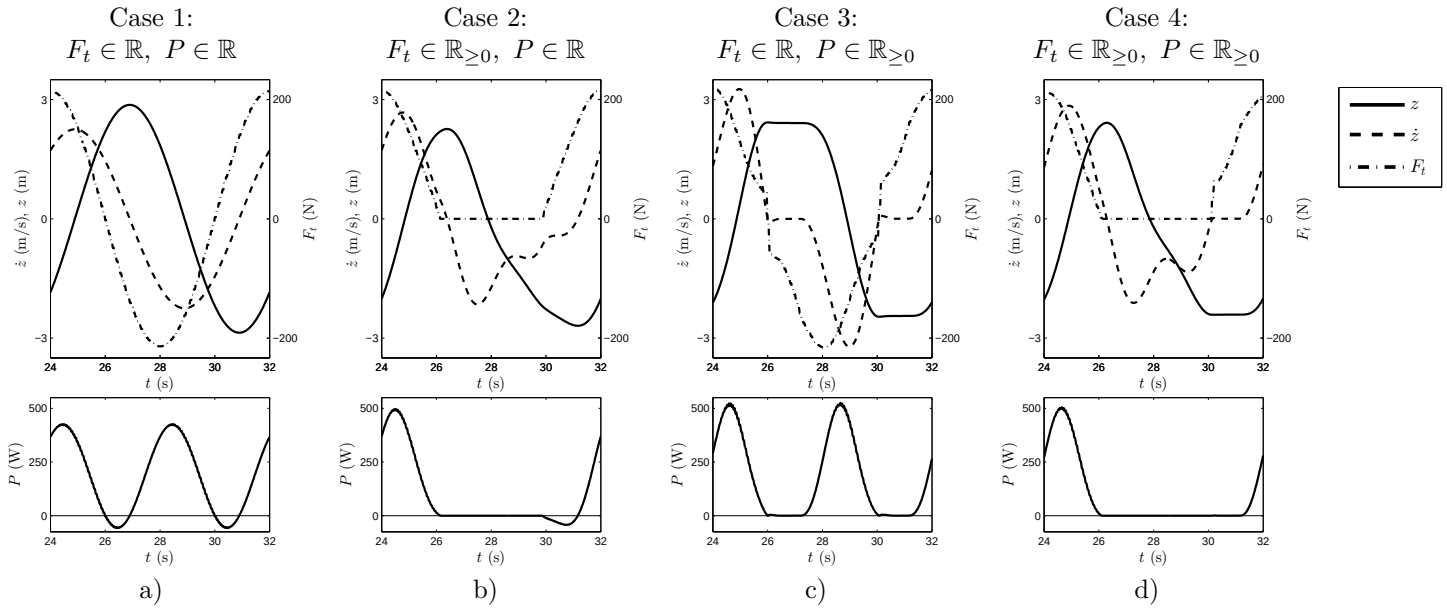

Figure 2: WEC optimal control results using DT for all four force/power constraint combinations.

In Case 3 velocity is held at zero (latching) instead of force (declutching) to satisfy the power constraint. Trajectories plotted in the force-velocity space provide an alternative visualization of this phenomenon. The force-velocity curves for all four cases are plotted Fig. 3. Case 3 is constrained from entering the upper-left or lower-right quadrants (where $P < 0$). Observe how this trajectory approaches the origin: velocity is brought to zero before passing through, rather than force being brought to zero. The horizontal shape of this trajectory near the origin is indicative of latching behavior.

One of the key observations here is that latching behavior emerged when the power constraint was imposed. There are no direct restrictions on $F_t(t)$ in Case 3, yet during certain periods the optimal force was found to be exactly the force that prevented any motion. To some extent this validates the latching control strategy. In all cases the velocity appeared to be in phase with wave elevation, agreeing with the phase requirement discussed above.

In Case 3 latching occurs both with $z > 0$ and $z < 0$, whereas in Case 4 the tether force constraint prevents any latching behavior when $z > 0$. In Case 4 latching is only possible when buoyancy force pushes the cylinder up (i.e., $z < z_0$). In the optimal solution for Case 4 latching does not occur.

Declutching behavior can also be identified easily from Fig. 3. Instead of passing through the origin horizontally as in latching, declutching is evidenced by vertical trajectories along the $F_t = 0$ axis (Cases 2 and 4). Case 2 is constrained to the right-hand plane, so spends some time along the $F_t = 0$ axis. Case 4, however, has a more interesting set of constraints. It must remain in the upper-right quadrant, unless $F_t = 0$. When tether force is zero velocity can be negative, and the trajectory moves down and back up the $F_t = 0$ axis as the heaving cylinder exhibits passive dynamic behavior.

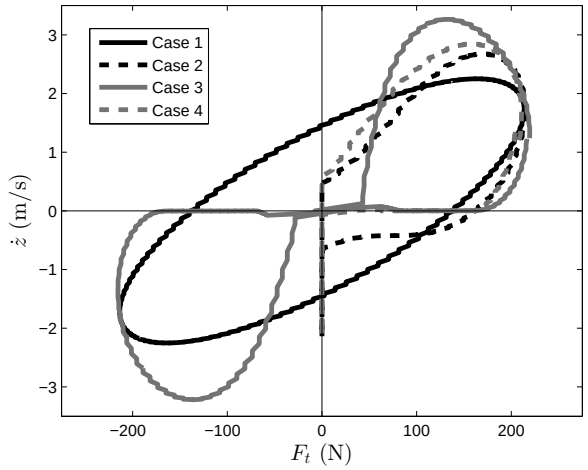

Figure 3: Velocity-Force curves for the four test cases.

The computational expense for all four cases was significantly different. Without power constraints the problem is a QP, and can be solved very efficiently (on the order of a few seconds with serial computing). With power constraints solution time is on the order of 10^2 – 10^3 seconds. Also, including the tether force constraint reduced computation time, both with and without the power constraint.

2.2.2 Parametric Studies Two parametric studies were performed: one on the number of time steps to explore convergence to a particular solution, and another on cylinder mass to identify a physical system design that provides maximum power production.

The number of time steps was varied from 721 to 1921. Energy extraction decreased slightly as the number of time steps was increased, but converged to a value before the maximum n_t value was reached. The total deviation in the objective function was approximately 4%. The value for n_t used in the above studies and in the mass parametric study below was large enough to provide accurate results (within 1% of the converged objective function value), while being low enough to enable efficient solution.

In the mass parametric study the cylinder mass was varied from 150 to 250 kg for Cases 1 and 2, and the results are shown in Fig. 4. The mass required to resonate with incoming waves, calculated using Eqn. (3), is 208 kg, and the trajectories that correspond to this mass in Figs. 4a and 4c are indicated with a dashed line. Power peak location and phase shift vary continuously with mass. Dramatic changes occur in peak power with Case 1, with the lowest peak power corresponding to the resonant mass. The power trajectories for the resonant masses have a fundamentally different shape than the others. In addition, the first position of peak power is the same for Cases 1 and 2.

Figs. 4b shows the total energy extraction for each case as mass is varied, where the resonant mass is indicated with a vertical line. Maximum energy extraction for Case 2 is closely aligned with the resonant mass, whereas for Case 1 the best energy production was found with a substantially different mass value.

3 Conclusion

Wave energy converters are an important potential renewable energy source. A significant amount of work has been performed with the objectives of improving WEC energy harvesting capability and cost-effectiveness. Most previous studies regarding WEC control have made significant assumptions about the nature of PTOs or other elements of WECs. While this eases solution and provides important insight, these assumptions restrict energy production potential and limit additional potential insights. We applied direct transcription, an open-loop optimal control method that places no unnecessary restrictions on control inputs, to WEC control design. We used F_t as the control input, making no assumptions regarding PTO structure or control trajectory. For linearly-constrained problems direct transcription enables very efficient solution, but also permits solution of problems with significant nonlinearities, singular optimal control problems, and problems with inequality path constraints. Even with no specification for using latching control in the problem definition, latching behavior emerged for the cases with power constraints. Declutching behavior only resulted when tether force constraints prevented pushing on the heaving cylinder (in other words, the tether went slack). Declutching did not arise as a technique for improving energy extraction. This initial application of DT to WECs highlights its potential for solving challenging control and co-design problems in this area.

REFERENCES

[1] Budal, K., and Falnes, J., 1975. "A resonant point absorber of ocean-wave power". *Nature,* **256**(5517), pp. 478–479.

[2] Erikkson, M., 2007. "Modeling and Experimental Verification of Direct Drive Wave Energy Conversion". Ph.D. dissertation, Uppsala University.

[3] Falnes, J., 2007. "A review of wave-energy extraction". *Marine Structures,* **20**(4), Oct., pp. 185–201.

[4] Falcão, A. F. d. O., Justino, P. A. P., Henriques, J. a. C. C., and André, J. M. C. S., 2009. "Reactive versus Latching Phase Control of a Two-body Heaving Wave Energy Converter". In the Proceedings of the European Control Conference.

[5] Drew, B., Plummer, A., and Sahinkaya, M., 2009. "A review of wave energy converter technology". In the Proceedings of the Institution of Mechanical Engineers, Part A: Journal of Power and Energy, Vol. 223, pp. 887–902.

[6] Scruggs, J. T., 2011. "Multi-Objective Optimal Causal Control of an Ocean Wave Energy Converter in Random Waves". In OCEANS 2011, IEEE, pp. 1–6.

[7] Lattanzio, S. M., and Scruggs, J. T., 2011. "Maximum power generation of a wave energy converter in a stochastic environment". In the 2011 IEEE International Conference on Control Applications (CCA), IEEE, pp. 1125–1130.

[8] Korde, U., 2000. "Control system applications in wave energy conversion". In the Proceedings of the OCEANS 2000 MTS/IEEE Conference and Exhibition, Vol. 3, pp. 1817–1824.

[9] Clément, A. H., and Babarit, A., 2012. "Discrete control of resonant wave energy devices". *Philosophical Transactions of the Royal Society A: Mathematical, Physical and Engineering Sciences,* **370**(1959), Jan., pp. 288–314.

[10] Budal, K., and Falnes, J., 1980. "Interacting point absorbers with controlled motion". In *Power from Sea Waves*, B. Count, ed. Academic Press, pp. 381–399.

[11] Falnes, J., 2002. *Wave-Energy Absorption by Oscillating Bodies.* Cambridge University Press.

[12] Pitti, A., and Lungarella, M., 2006. "Exploration of Natural Dynamics Through Resonance and Chaos". In the Proceedings of the 9th Conference on Intelligent Autonomous

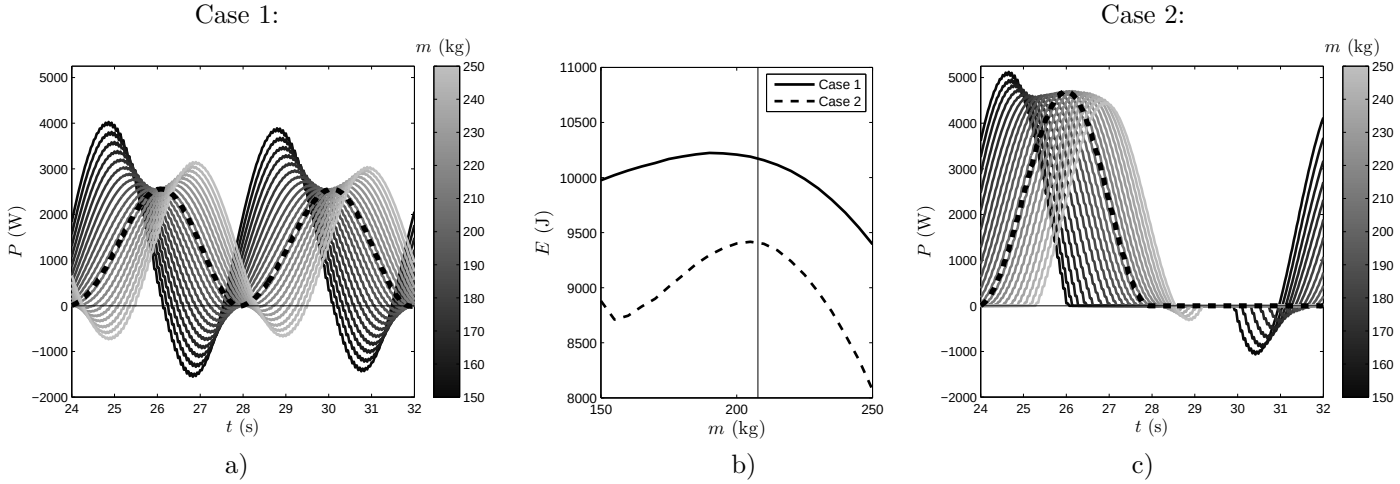

Figure 4: Parametric study on cylinder mass.

Systems, pp. 558–565.

[13] Allison, J., 2012. "Engineering System Co-Design with Limited Plant Redesign". In the Proceedings of the 8th AIAA Multidisciplinary Design Optimization Specialist Conference.

[14] Allison, J., 2012. "Plant-Limited Co-Design of an Energy Efficient Counterbalanced Robotic Manipulator". In the Proceedings of the 2012 ASME Design Engineering Technical Conference.

[15] McCormick, M., 1981. *Oceans Wave Energy Conversion*. Wiley.

[16] Fathy, H., 2003. "Combined Plant and Control Optimization: Theory, Strategies and Applications". Ph.D. dissertation, University of Michigan.

[17] Allison, J., and Nazari, S., 2010. "Combined Plant and Controller Design Using Decomposition-Based Design Optimization and the Minimum Principle". In the Proceedings of the 2010 ASME Design Engineering Technical Conference.

[18] Allison, J., and Han, Z., 2011. "Co-Design of an Active Suspension Using Simultaneous Dynamic Optimization". In the Proceedings of the 2011 ASME Design Engineering Technical Conference.

[19] Vantorre, M., Banasiak, R., and Verhoeven, R., 2004. "Modelling of hydraulic performance and wave energy extraction by a point absorber in heave". *Applied Ocean Research,* **26**(1-2), Feb., pp. 61–72.

[20] Engstrom, J., Kurupath, V., Isberg, J., and Leijon, M., 2011. "A Resonant Two Body System for a Point Absorbing Wave Energy Converter With Direct-Driven Linear Generator". *Journal of Applied Physics,* **110**(12), p. 124904.

[21] Ivanova, I. A., Bernhoff, H., Ågren, O., and Leijon, M., 2005. "Simulated generator for wave energy extraction in deep water". *Ocean Engineering,* **32**(14-15), Oct., pp. 1664–1678.

[22] Eidsmoen, H., 1996. Simulation of a slack-moored heaving-buoy wave-energy converter with phase control. Tech. rep., Norwegian University of Science and Technology.

[23] de O Falcão, A. F., 2007. "Modelling and control of oscillating-body wave energy converters with hydraulic power take-off and gas accumulator". *Ocean Engineering,* **34**(14-15), Oct., pp. 2021–2032.

[24] Falcão, A. F. D. O., 2008. "Phase control through load control of oscillating-body wave energy converters with hydraulic PTO system". *Ocean Engineering,* **35**(3-4), Mar., pp. 358–366.

[25] Santana, A. G., El, D., Andrade, M., De, A., Jaén, V., and Ingeniería, A. G., 2010. "Control of Hydrodynamic Parameters of Wave Energy Point Absorbers using Linear Generators and VSC-based Power Converters Connected to the Grid". In the International Conference on Renewable Energies and Power Quality.

[26] Falnes, J., and Hals, J., 2012. "Heaving buoys, point absorbers and arrays". *Philosophical Transactions of the Royal Society A: Mathematical, Physical and Engineering Sciences,* **370**(1959), Jan., pp. 246–77.

[27] Ringwood, J., and Butler, S., 2004. "Optimisation of a wave energy converter". In the Proceedings of the IFAC Confernece On Control Applications in Marine Systems, pp. 155–160.

[28] Pontryagin, L., Boltyanskii, V., Gamkrelidze, R., and Mishchenko, E., 1962. *The mathematical theory of optimal processes (International series of monographs in pure and applied mathematics)*. Interscience Publishers.

[29] Hals, J., Falnes, J., and Moan, T., 2011. "Constrained Optimal Control of a Heaving Buoy Wave-Energy Converter". *Journal of Offshore Mechanics and Arctic Engineering,* **133**(1), p. 011401.

[30] Amon, E. A., Schacher, A. A., and Brekken, T. K. A., 2009. "A Novel Maximum Power Point Tracking Algorithm for Ocean Wave Energy Devices". In the Energy Conversion Congress and Exposition, IEEE, pp. 2635–2641.

[31] Valério, D., Beirão, P., and Sá da Costa, J., 2007. "Optimisation of wave energy extraction with the Archimedes Wave Swing". *Ocean Engineering,* **34**(17-18), Dec., pp. 2330–2344.

[32] Hoskin, R., Count, B., Nichols, N., and Nichol, D., 1986. "Phase control for the oscillating water column". In *Hydrodynamics of Ocean Wave-Energy Utilization*, D. Evans and A. F. de O Falcão, eds. Springer, Berlin, pp. 257–268.

[33] Fusco, F., and Ringwood, J., 2011. "Suboptimal Causal Reactive Control of Wave Energy Converters Using a Second Order System Model WEC". In the Proceedings of the 21st International Offshore (Ocean) and Polar Engineering Conference.

[34] Garnaud, X., 2010. "Comparison of wave power extraction by a compact array of small buoys and by a large buoy". *IET*

Renewable Power Generation, **4**(6), p. 519.
[35] Falnes, J., 1980. "Radiation impedance matrix and optimum power absorption for interacting oscillators in surface waves". *Applied Ocean Research,* **2**(2), Apr., pp. 75–80.
[36] De Backer, G., Vantorre, M., and Rouck, J. D., 2009. "Wave energy absorption by point absorber arrays". In *Book of abstracts: an overview of marine research in Belgium anno 2009. 10th VLIZ Young Scientists' Day. Special edition at the occasion of 10 years VLIZ.*, J. Mees, ed. VLIZ, p. 37.
[37] Biegler, L. T., 2010. *Nonlinear Programming: Concepts, Algorithms, and Applications to Chemical Processes.* SIAM.
[38] Cramer, E. J., Dennis, J. E., Frank, P. D., Lewis, R. M., and Shubin, G. R., 1994. "Problem formulation for multidisciplinary optimization". *SIAM Journal of Optimization,* **4**, pp. 754–776.
[39] Betts, J. T., 2010. *Practical Methods for Optimal Control and Estimation Using Nonlinear Programming.* SIAM.
[40] Hoerner, S., 1965. *Fluid Dynamic Drag.* Hoerner Fluid Dynamics.
[41] Feehery, W. F., and Barton, P. I., 1998. "Dynamic optimization with state variable path constraints". *Computers & Chemical Engineering,* **22**(9), pp. 1241–1256.
[42] Boyd, S., and Vandenberghe, L., 2004. *Convex Optimization.* Cambridge University Press.